Scientific Research Publishing

Open Journal of Forestry, 2026, 16(1), 83-105
https://www.scirp.org/journal/ojf
ISSN Online: 2163-0437
ISSN Print: 2163-0429

High-Resolution Study of the Late Holocene from Pollen of a Marine Core in the Gulf of Guinea (Cameroon): Paleoenvironmental and Ecological Dynamics in Central Africa during the Last 2,500 Years

Martin Darius Bengo[1], Hugues-Yvan Gomat[1,2], Alain Mercier Bita[3], Suspense Averti Ifo[1,2], Jean Maley[4], Pierre Giresse[5]

[1]Ecole Normale Supérieure, Université Marien Ngouabi, Brazzaville, Congo
[2]Laboratoire de Télédétection et d'Écologie Forestière, Université Marien Ngouabi, Brazzaville, Congo
[3]Ecole Nationale Supérieure d'Agronomie et de Foresterie, Université Marien Ngouabi, Brazzaville, Congo
[4]Sciences et Techniques, Université Montpellier 2, Montpellier, France
[5]CEFREM, UMR 5110 CNRS, Université de Perpignan via Domitia, Perpignan, France
Email: dmbengo@yahoo.fr, dmbengo@gmail.com

How to cite this paper: Bengo, M. D., Gomat, H.-Y., Bita, A. M., Ifo, S. A., Maley, J., & Giresse, P. (2026). High-Resolution Study of the Late Holocene from Pollen of a Marine Core in the Gulf of Guinea (Cameroon): Paleoenvironmental and Ecological Dynamics in Central Africa during the Last 2,500 Years. *Open Journal of Forestry, 16,* 83-105.
https://doi.org/10.4236/ojf.2026.161006

Received: December 13, 2025
Accepted: January 10, 2026
Published: January 13, 2026

Abstract

A high-resolution palynological study was conducted on marine core CF collected at 38 m water depth on the Cameroonian continental shelf (Gulf of Guinea). Litho-sedimentary analysis distinguishes two major depositional units, reflecting shifts from dynamic to calmer marine environments. Four radiocarbon dates establish a robust age-depth model spanning the last 2,500 years. Twenty samples were analyzed following standard palynological procedures, with a minimum count of 300 pollen grains per sample. A total of 228 taxa belonging to 90 plant families were identified. Rhizophora pollen dominates the assemblages, followed by spores, Poaceae, Alchornea, Cyperaceae, and Elaeis. Pollen diagrams and correspondence factor analysis reveal three major vegetation phases: 1) a forest-dominated phase, 2) an expansion of herbaceous savannas culminating in a Late Holocene savanna optimum between ~1,600 and 900 cal yr BP, and 3) a phase of forest recovery characterized by pioneer taxa. These vegetation changes reflect the combined influence of regional climatic variability, coastal dynamics, and increasing human pressure. The CF marine record provides a key reference for understanding Late Holocene land-sea interactions and ecosystem sensitivity in Central Africa.

Keywords

Palynology, Late Holocene, Gulf of Guinea, Marine Sediments, Vegetation Dynamics, Climate Variability, Central Africa

1. Introduction

Understanding long-term interactions between climate variability, vegetation dynamics, and human activities is essential for assessing the resilience of tropical ecosystems under current and future environmental change. Recent assessments highlight accelerating anthropogenic impacts on climate systems, including warming, altered precipitation regimes, and increasing coastal vulnerability (IPCC, 2021; Malhi et al., 2014). In tropical regions, such changes can modify forest-savanna boundaries, sediment fluxes, and coastal environments, particularly in areas influenced by major river systems and monsoon-driven circulation, such as the Gulf of Guinea.

Paleoenvironmental archives provide a unique opportunity to place recent environmental changes into a long-term perspective. Among these archives, pollen preserved in continental and marine sediments constitutes one of the most widely used proxies for reconstructing past vegetation and climate variability (Faegri & Iversen, 1992). Palynological records allow the identification of major ecological shifts, including forest contraction and expansion, savanna development, and the response of ecosystems to climatic oscillations and anthropogenic disturbances over millennial timescales (Maley, 1991; Maley et al., 2018).

In the countries bordering the Gulf of Guinea, numerous palynological studies based on continental archives—especially lake sediments—have reconstructed Holocene vegetation history. Key West African sites include Lake Bosumtwi (Maley, 1991; Julier et al., 2018), Lake Sélé (Salzmann & Hoelzmann, 2005; Bremond et al., 2017), and Lake Tilla (Salzmann et al., 2002). In Central Africa, records from Gabon (Ngomanda et al., 2005; Giresse et al., 2009; Ngomanda et al., 2009a; Ngomanda et al., 2009b), Congo (Elenga & Vincens, 1990; Elenga et al., 1996; Vincens et al., 1994; Elenga et al., 1996; Brncic et al., 2009; Maley & Willis, 2010), and the Democratic Republic of Congo (Kiahtipes & Schefuss, 2018) document major Late Holocene reorganizations. Many of these sequences report forest fragmentation and savanna expansion episodes around 3,200-2,500 cal yr BP at the regional scale (Maley et al., 2018; Giresse et al., 2020).

In Cameroon, palynological investigations span a wide range of ecological settings, from high-altitude sites (e.g., Lake Bambili and Shum Laka) to lowland and coastal environments (Assi-Kaudjhis et al., 2008; Assi-Kaudjhis et al., 2010; Assi-Kaudjhis, 2012; De Maret et al., 1987; Moyersons, 1996). Low-altitude archives include Lake Barombi-Mbo (Maley & Brenac, 1998; Lebamba et al., 2012), Lake Ossa (Reynaud-Farrera et al., 1996; Giresse et al., 2005; Nguetsop et al., 2010), Lake Mbalang (Vincens et al., 2010), Lake Njupi (Zogning et al., 1997),

and the Nyabessan swamps (Giresse et al., 2009). While these continental archives provide detailed local records, they can be influenced by site-specific factors (basin morphology, hydrology, catchment-scale processes). In contrast, marine sediment cores collected on the continental shelf integrate pollen signals over large drainage basins and coastal zones, offering a regional perspective on vegetation dynamics and land-sea interactions (Bengo & Maley, 1991; Bengo et al., 2020).

Despite their high potential, palynological studies of marine cores from the Cameroonian continental shelf remain relatively scarce. In the Gulf of Guinea, marine palynological records have documented vegetation and climate variability over longer timescales, including cores off Liberia (Jahns et al., 1998), Côte d'Ivoire (Fredoux, 1994; Lézine & Cazet, 2005), Ghana (Lézine & Vergnaud-Grazzini, 1993), Niger (Dupont & Weinelt, 1996), Gabon (Dupont et al., 1998), Congo (Jahns, 1996; Bengo & Maley, 1991), and Angola (Shi & Dupont, 1997). Along the Cameroonian margin, previous work on core C61 has highlighted major Late Quaternary vegetation changes (Bengo, 1996; Bengo et al., 2025b), and dinocyst data from core GeoB4905 also illustrate land-ocean interactions in the region (Marret et al., 2013). However, limited sampling density in the uppermost sections of some marine cores can restrict detailed interpretations of Late Holocene variability.

In this context, the present study focuses on the CF marine core collected at a 38 m water depth on the Cameroonian continental shelf near the Bay of Douala (Ngueutchoua, 1996; Giresse et al., 1995). The base of CF overlaps with the top of core C61, enabling a high-resolution investigation of vegetation and environmental changes over the last ~2,500 years. By combining litho-sedimentary observations, radiocarbon dating, detailed pollen analysis, and multivariate statistics, this study aims to: 1) reconstruct Late Holocene vegetation dynamics in Central Africa; 2) identify phases of forest and savanna expansion and regression; and 3) assess the respective roles of climatic variability, coastal processes, and human activities in shaping regional ecosystems.

This marine record provides new insights into Late Holocene land-sea interactions in the Gulf of Guinea and contributes to a better understanding of the sensitivity of Central African ecosystems to environmental change.

2. Geographical and Environmental Context

2.1. Geographical Location

The Atlantic coast of Cameroon is located in the innermost part of the Gulf of Guinea, within the Bay of Biafra, between latitudes 2˚20'N and 4˚30'N and longitudes 8˚20'E and 9˚55'E (**Figure 1**). The continental shelf extends seaward for approximately 30 km - 50 km from the coastline, reaching depths of about 200 m. The Cameroonian shelf, oriented predominantly north-south, is characterized by two sectors of unequal extent. Beyond depths of 100 m - 200 m, the continental slope steepens markedly, and isobaths become closely spaced.

The coastline displays strong geomorphological contrasts from north to south. Four major coastal landscapes can be distinguished: 1) a low-lying mangrove coast associated with the Niger Delta system, corresponding to the estuarine complexes of the Rio del Rey and Cross River; 2) a rocky volcanic coast formed by lava flows from Mount Cameroon, characterized by small basaltic cliffs; 3) a second low mangrove coast in the Bay of Douala, also known as the "Bouches du Cameroun," a funnel-shaped embayment approximately 30 km long and 50 km wide that receives several major rivers; and 4) a long sandy coastline extending from the Sanaga estuary to Campo, composed of alternating beaches and rocky headlands, with parallel lagoons developed landward of barrier beaches.

The continental shelf is widest in the northern sector, reaching up to 80 km, and progressively narrows southward where it intersects the Precambrian basement. Shelf widenings correspond to major Miocene and Plio-Pleistocene progradational phases. Two major sedimentary basins border the Cameroonian coast: the Douala-Rio del Rey Basin to the north, extending between the 2nd and 5th parallels north and divided by the Cameroon Volcanic Line into the Douala sub-basin (≈7,000 km^2) to the east and the Rio del Rey sub-basin (≈2,500 km^2) to the west; and the Campo Basin to the south, which represents the northern extension of the Gabon-Equatorial Guinea Basin.

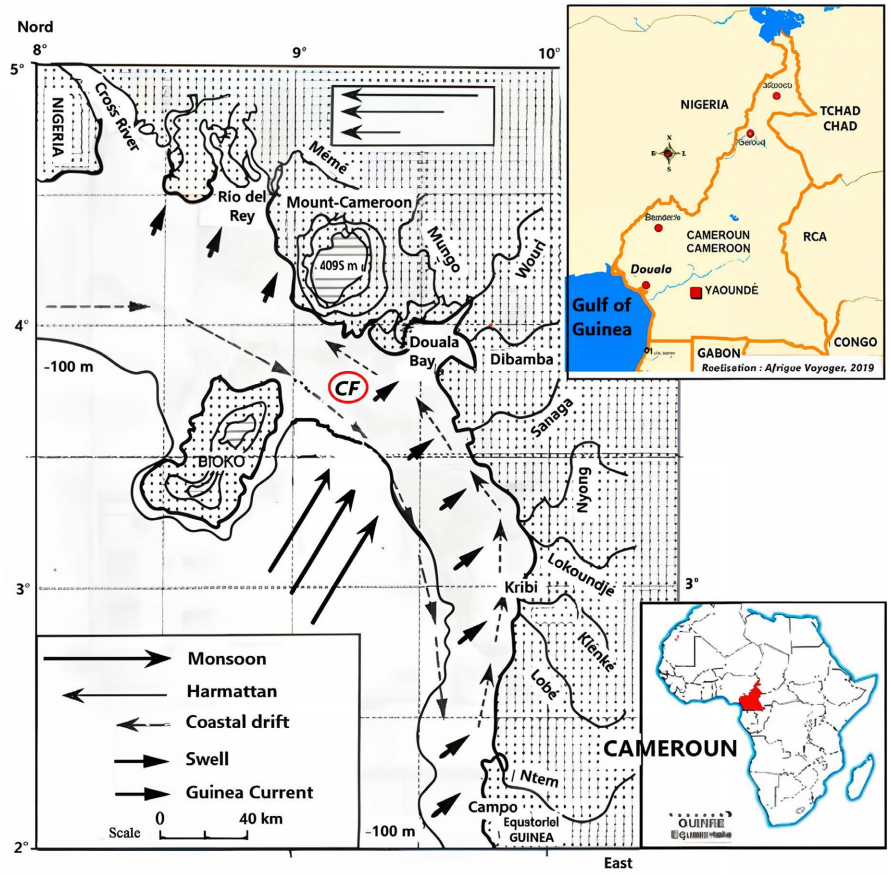

Figure 1. Location of the sampling site on the Cameroonian continental shelf.

2.2. Marine Environmental Context

2.2.1. Oceanographic Setting

Ocean circulation in the northern Gulf of Guinea is mainly controlled by the combined effects of wave action and tidal currents (Bourlès et al., 1999; Braga et al., 2004; Kolodziejczyk, 2008). Along the southern Cameroonian coast, tidal amplitudes remain relatively low, reaching approximately 1.5 m at Kribi and 1.8 m at Campo. In contrast, they increase to about 2 m in the Bay of Douala and up to 3 m in the shallow, open Rio del Rey estuary.

Ocean swells predominantly originate from the WSW-SW sector. They strike the coastline almost perpendicularly between the Sanaga estuary and the Rio del Rey, while approaching the southern coast at a more oblique angle. This configuration generates a strong longshore drift responsible for the development of northward-oriented coastal spits at the mouths of the Nyong and Sanaga rivers and within the Bay of Douala (Giresse et al., 1995).

The main surface circulation influencing the study area corresponds to the Guinea Current, which is an extension of the North Equatorial Countercurrent. This current flows southward along the Cameroonian margin and plays a key role in the redistribution of fine-grained sediments and organic particles on the continental shelf. The combined action of the equatorial countercurrent, the Guinea Current, and coastal drift contributes to the dispersal of terrigenous and biogenic material derived from recent sedimentary inputs (Bengo et al., 2025a).

2.2.2. Sediments of the Cameroonian Continental Shelf

Sedimentation on the Cameroonian continental shelf comprises both ancient and modern deposits. Recent sediments are adjusted to present-day hydrodynamic conditions, whereas older deposits originate from former marine environments and may have undergone phases of emergence, reworking, and compaction. From a chronological perspective, the sedimentary record includes remnants of low sea-level stages, deposits associated with the Holocene transgression, and sediments formed under the influence of modern hydrodynamics.

Four main sedimentary facies are recognized: 1) quartz-rich sands developed in the deltas of the Sanaga and Nyong rivers; 2) organogenic sands composed of calcareous bioclasts, particularly abundant near Kribi; 3) fine-grained muds dominated by lutites (>75%), extensively covering the northern shelf and composed mainly of kaolinite, smectite, and illite; and 4) glauconitic sands formed by polychaete fecal pellets along the outer shelf margin. The spatial distribution of clay minerals shows a dominance of kaolinite in the southern sector, smectites influenced by the Guinea Current in the northwest, and illites in the northern shelf. Interactions between recent fluvial inputs and reworked pre-Holocene sediments generate a complex sedimentary system.

2.3. Continental Environmental Context

2.3.1. Geological, Pedological, and Geomorphological Framework

The Cameroonian continental margin is a geological structure inherited from the

opening of the South Atlantic during the Early Cretaceous, characterized by N60-oriented fault systems that produced alternating horst and graben structures (Aloisi et al., 1995). In marine settings, sedimentation is dominated by recent deltaic deposits in the north, whereas relict glauconitic and bioclastic sands prevail in the southern sector, representing remnants of the Last Glacial Maximum and subsequent Holocene transgressions (Giresse et al., 1995).

On land, the humid equatorial zone of southern Cameroon is dominated by kaolinite-rich ferralitic soils developed on Precambrian basement rocks. Hydromorphic soils enriched in organic matter occur in swampy lowlands, while volcanic regions in western and southwestern Cameroon are characterized by Andosols derived from basic volcanic materials (Martin, 1966; Segalen, 1967). The stepped continental relief, extending from the coastal plain to the Adamawa Plateau, promotes intense erosion and facilitates rapid transfer of terrigenous material toward the marine environment.

2.3.2. Present Climate and Vegetation

The climate of coastal Cameroon is largely controlled by the seasonal migration of the Intertropical Convergence Zone (ITCZ), which governs the alternation between a humid season dominated by oceanic monsoon air masses and a dry season influenced by continental trade winds (Leroux, 1983; Piton, 1987; Suchel, 1988). Two main climatic domains are distinguished: an equatorial climate in southern Cameroon, characterized by high temperatures, high humidity, and two rainy and two dry seasons, and a tropical climate in the north with one rainy season and one dry season (Suchel, 1988).

Rainfall is particularly abundant along the coast, exceeding 10,000 mm locally around Douala and Mount Cameroon. These humid conditions favor the development of dense evergreen forests dominated by taxa such as Sacoglottis, Lophira, Caesalpiniaceae, and Sapotaceae (Letouzey, 1968). Northward, vegetation gradually transitions to semi-deciduous forests and then to Sudanian savannas dominated by Poaceae, Cyperaceae, Combretaceae, Bridelia, and Hymenocardia, followed by Sahelian savannas beyond the Adamawa Plateau. Mangrove ecosystems dominated by Rhizophora develop along sheltered coastal zones and estuaries (Boyé et al., 1975; Din, 1991), while montane forests characterized by Podocarpus occur at higher elevations.

The present floristic composition is reflected in pollen assemblages preserved in marine sediments, providing a key reference for Holocene paleoenvironmental reconstructions (Bengo et al., 2020; Bengo et al., 2025a). Intense rainfall combined with stepped topography results in strong soil erosion and efficient transport of clays, silts, and pollen grains toward the continental shelf.

2.3.3. River Systems and Their Role in Modern Sedimentation

The northern sector of the Cameroonian continental shelf is influenced by the Niger Delta complex, which includes the Niger River and associated coastal rivers of the Lagos region and delivers large volumes of freshwater and sediment to the

Gulf of Guinea. Several rivers draining the volcanic slopes of Mount Cameroon feed the mangrove systems of the Rio del Rey. In the Bay of Douala, river discharge is irregular, with major contributions from the Mungo, Wouri, and Dibamba rivers (Mahé & Olivry, 1991).

The Sanaga River is the principal fluvial system supplying the Cameroonian shelf. With a drainage basin of approximately 135,000 km^2, it originates on the Adamawa Plateau and traverses savanna, semi-deciduous forest, and evergreen forest zones before reaching the coast. Its major tributary, the Mbam River, drains intensively cultivated areas of the Bamileke highlands. Further south, the Nyong and Ntem rivers exhibit equatorial hydrological regimes with pronounced floods during spring and autumn. The Sanaga basin accounts for the majority of terrigenous inputs to the shelf, with specific erosion rates reaching about 44 t km^{-2} yr^{-1}, corresponding to nearly 6 million tons of sediment transported annually to the ocean.

3. Materials and Methods

3.1. Core Location and Sampling Strategy

The CF marine core was collected on the Cameroonian continental shelf at a water depth of 38 m off the Bay of Douala, upstream of the C61 core site, at coordinates 3˚40'05"N and 9˚11'02"E (**Figure 2**). The core is located within the Holocene High-Level Prism (HLP). Sedimentation in this area mainly reflects terrigenous inputs from coastal rivers, particularly the Sanaga River, combined with in situ biogenic production (Ngueutchoua & Giresse, 2010).

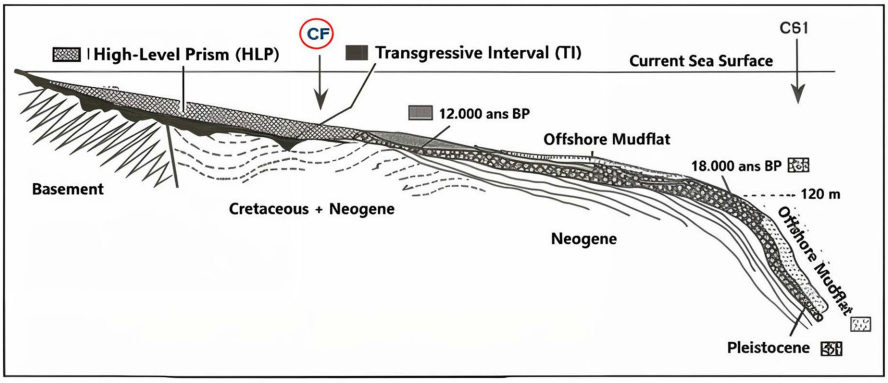

Figure 2. Location of the CF core on the Cameroonian continental shelf.

A total of 20 samples were collected along the 260 cm-long core. Eight samples were taken at 20 cm intervals in the upper section (0 cm - 140 cm), characterized by relatively low sedimentation rates, while twelve samples were collected at the same interval in the lower section (140 m - 260 cm), where sedimentation was more rapid. This sampling strategy provides a temporal resolution of approximately 5 cm per 20 years in the lower part of the core and allows detailed reconstruction of Late Holocene paleoenvironmental variability.

3.2. Palynological Methods

3.2.1. Sample Processing

Palynological preparation followed standard procedures for marine sediments (Faegri & Iversen, 1992; Riding, 2021). Samples were treated chemically to remove carbonates, silicates, and extraneous organic matter, followed by repeated washing and centrifugation. The final residues were mounted on microscope slides using glycerine jelly, ensuring optimal preservation and visibility of pollen grains and spores.

3.2.2. Pollen Identification and Classification

Pollen and spores were observed under an optical microscope at magnifications ranging from × 400 to × 1000. A minimum of 300 grains per sample was counted to ensure statistical reliability. Taxonomic identification was based on published pollen atlases (Maley, 1970; Bonnefille & Riollet, 1980; Salard-Cheboldaeff, 1980; Salard-Cheboldaeff, 1981; Salard-Cheboldaeff, 1982; Salard-Cheboldaeff, 1983) and on the modern reference collection of the Palynology Laboratory at the University of Montpellier. Identified taxa were grouped according to their ecological affinities, including dense evergreen forests, semi-deciduous forests, savannas, Afro-montane vegetation, and mangroves.

3.2.3. Pollen Diagrams and Ecological Interpretation

In tropical marine sediments, Rhizophora pollen and spores are often overrepresented. To better assess the continental vegetation signal, pollen diagrams were constructed using two datasets: one including all taxa and another excluding Rhizophora and spores. Paleoenvironmental interpretation was based on indicator taxa reflecting climatic and ecological conditions. Poaceae and Bridelia are indicative of dry savanna phases, whereas Caesalpiniaceae, Sapotaceae, and Pycnanthus reflect humid forest conditions. Podocarpus is associated with cooler climatic conditions at higher elevations. Combined with the chronological framework, these indicators allow the reconstruction of Late Holocene environmental changes and correlation with regional and global climatic variability.

4. Results

4.1. Litho-Sedimentary Characteristics and Chronology of Core CF

The lithological profile of core CF (**Figure 3**) reveals two main sedimentary units, previously described by Ngueutchoua (1996). The upper unit (0 cm - 180 cm) consists of homogeneous grey-green mud containing rare mollusc fragments, indicating deposition under low-energy and relatively stable environmental conditions (**Figure 3**). In contrast, the lower unit (180 cm - 260 cm) is composed of grey-green, slightly sandy clayey mud with millimetre-sized quartz grains, abundant mollusc debris, and numerous fecal pellets (coprolites), reflecting a more energetic depositional environment (**Figure 3**).

Clay mineral assemblages are dominated by kaolinite, with subordinate smectite and illite, indicating a predominantly continental origin of detrital material,

mainly supplied by the Sanaga River basin. In the sandy lower unit, geochemical analyses show elevated concentrations of magnetic iron and calcium carbonate ($CaCO_3$). Organic carbon content is generally low throughout the sequence but increases progressively toward the upper part of the core, suggesting enhanced marine productivity and environmental stabilization during the most recent depositional phases (Figure 3).

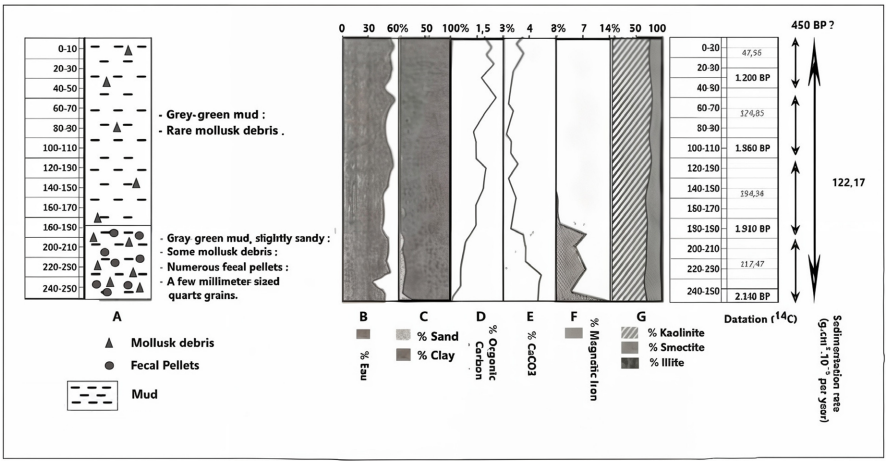

Figure 3. Lithological profile of core CF (adapted from Ngueutchoua, 1996).

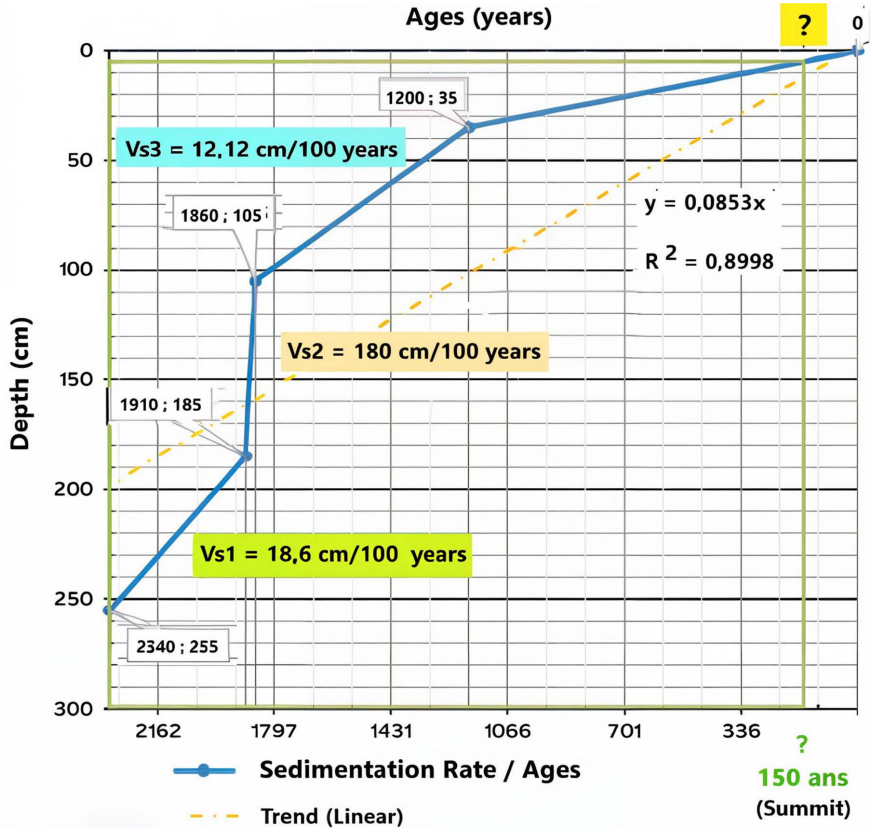

Figure 4. Age-depth model and sedimentation rates derived from calibrated ^{14}C dates (Bengo, 1996).

Chronological control is based on four radiocarbon (^{14}C) dates obtained from bulk organic matter and mollusc shells (Ngueutchoua, 1996; Giresse et al., 1995). These dates were used to construct an age-depth model and estimate sedimentation rates (Figure 4). Ages for undated intervals were interpolated linearly between dated levels to provide a continuous chronological framework for palynological interpretation (Figure 4). According to this model, the uppermost 10 cm of the core corresponds to approximately the last 150 years (Figure 4).

Sedimentation rates vary markedly through time (Figure 4). Between ~2,340 and 1,910 cal yr BP, the mean sedimentation rate was about 18.6 cm per 100 years. A short interval between ~1,910 and 1,860 cal yr BP is characterized by exceptionally rapid accumulation, reaching nearly 1 m within approximately 50 years. Subsequently, from ~1,860 to 1,200 cal yr BP, sedimentation rates decreased sharply to about 12.1 cm per 100 years.

4.2. Pollen Identification, Abundance, and Taxonomic Diversity

Compared with offshore core C61, which already displays high pollen concentrations, core CF—collected closer to the coast—shows markedly higher pollen densities. Preliminary slide observations indicate an average of approximately 900 pollen grains per sample. The surface sample (0 cm - 10 cm) exhibits the lowest pollen concentration, whereas the level between 150 and 160 cm, dated to around 1,895 cal yr BP, contains the highest abundance (Table 1).

In total, 18,374 pollen and spore grains were identified. Among other palynomorphs, 249 grains were indeterminate, 81 were damaged, and only 33 corresponded to dinoflagellate cysts. The dataset includes 228 taxa belonging to 90 plant families. The assemblages are dominated by *Rhizophora* pollen (49.76%), followed by spores (17.42%), Poaceae (7.66%), *Alchornea* (3.72%), Cyperaceae (2.98%), and *Elaeis* (2.07%) (Table 1). The highest taxonomic richness is observed in Rubiaceae (26 genera), followed by Euphorbiaceae (17), Phyllanthaceae (11), and Caesalpiniaceae (9).

Table 1. Counts and percentages of the main pollen taxa and plant groups.

	LEVELS	0 - 10	10 - 20	20 - 30	40 - 50	60 - 70	80 - 90	100 - 110	120 - 130	140 - 150	150 - 160	160 - 170	170 - 180	180 - 190	190 - 200	200 - 210	210 - 220	220 - 230	230 - 240	240 - 250	250 - 260	Total					
Taxa/Ages	Total _Pollens	155	520	885	1270	1490	1675	1860	1875	1885	1890	1900	1905	1910	1970	2035	2095	2155	2215	2280	2340	Aver-age	Mini-muma	Maxi-mum	Occur-rence	Habi-tats	Plant_Type
														Base_1													
Rhizophora	9150	53.47	49.72	41.18	46.56	48.60	43.64	48.21	49.88	54.69	48.94	46.63	51.19	58.40	52.28	47.80	49.11	51.06	54.28	51.93	46.64	49.71	41.18	58.40	20	P_Ma	O_A/a
Spores	3212	16.33	14.95	18.28	15.61	15.83	16.49	20.03	20.10	12.20	18.41	21.07	17.10	16.69	20.00	20.30	16.61	15.49	16.38	16.57	19.04	17.37	12.20	21.07	20	P_F/S	O_H
GRAMINAE	1408	2.18	7.75	15.26	14.02	11.34	13.64	7.15	6.10	5.88	8.57	8.33	6.62	4.91	4.00	7.10	6.58	5.96	4.69	5.06	8.87	7.70	2.18	15.26	20	S	H
														Base_2													
GRAMINAE	1408	7.21	21.95	37.65	37.06	31.89	34.20	22.52	20.32	17.75	26.24	25.81	20.87	19.70	14.43	22.26	19.21	17.81	15.99	16.08	25.84	22.74	7.21	37.65	20	S	H
Alchornea type	685	19.82	10.63	8.24	8.39	8.27	5.54	10.36	8.37	10.92	12.78	14.64	11.88	13.79	12.94	15.05	10.98	9.67	13.45	11.99	11.80	11.48	5.54	19.82	20	F	a
CYPER-ACEAE	549	9.46	7.01	12.94	13.99	14.17	14.01	13.06	12.75	6.83	8.01	9.43	11.30	4.93	5.97	5.96	4.27	7.63	8.12	4.90	9.35	9.20	4.27	14.17	20	S	H
Pycnanthus	456	7.66	5.43	4.31	4.55	5.51	7.17	8.11	4.78	10.92	4.77	6.45	8.99	9.85	11.44	8.78	8.54	7.89	12.94	7.63	7.80	7.68	4.31	12.94	20	F	A
Elaeis guinensis	381	3.60	3.39	5.49	4.90	7.48	4.89	5.86	7.57	5.46	7.67	6.45	5.22	5.42	4.48	5.02	8.54	5.85	6.85	10.63	6.24	6.05	3.39	10.63	20	F/Cu	A

Continued

Uapaca	288	4.95	3.62	3.92	1.40	2.36	4.23	6.31	4.38	4.44	4.77	4.22	6.67	3.94	7.96	9.40	3.05	5.09	4.57	7.63	4.23	4.86	1.40	9.40	20	S/F	A
Drypetes ituriensis	188	3.15	4.52	3.53	4.20	0.39	0.00	1.80	3.19	4.44	1.87	1.74	0.87	5.91	2.99	6.58	9.15	4.07	1.52	2.45	3.34	3.29	0.00	9.15	19	F	A/a
Commelina	161	3.15	5.20	0.78	3.85	1.57	3.58	4.50	5.18	2.73	2.04	2.48	1.45	2.46	2.49	2.82	2.13	1.78	1.52	2.72	2.67	2.76	0.78	5.20	20	S	H
Tetrorchydium	135	1.35	3.62	3.14	1.05	1.57	0.98	0.45	3.19	1.71	2.56	1.74	2.32	2.96	1.00	2.51	2.44	1.53	2.03	3.00	3.56	2.13	0.45	3.62	20	F	a/A
Podocarpus	115	0.90	1.13	1.96	2.10	0.79	1.63	2.25	1.99	3.07	1.36	1.49	1.74	1.48	2.99	1.25	3.66	1.78	2.28	2.18	1.78	1.89	0.79	3.66	20	F	a
COMBRETACEAE	98	1.80	1.58	0.78	1.05	1.97	0.00	0.90	1.59	2.73	1.36	1.49	0.87	2.46	1.99	1.57	1.52	2.80	3.81	1.09	1.56	1.65	0.00	3.81	19	S/F	A/a/L
Mallotus	78	1.35	2.26	0.78	1.40	1.57	1.95	1.80	1.99	1.02	1.70	0.00	0.87	0.00	1.49	0.63	1.22	2.29	1.52	0.82	1.11	1.29	0.00	2.29	18	F/S	a
Lophira	77	1.35	0.00	1.18	0.00	0.79	0.65	1.35	0.80	1.71	1.19	2.48	0.87	2.46	1.00	0.94	1.83	2.80	2.03	1.36	0.67	1.27	0.00	2.80	18	S/F	A
COMPOSITAE	69	0.90	1.13	1.57	1.75	0.79	1.30	0.90	1.99	0.68	1.02	1.24	1.16	1.97	1.49	0.94	0.61	0.76	0.25	1.91	1.11	1.17	0.25	1.99	20	S	H
Irvingia	63	1.80	0.90	1.18	1.05	0.79	1.30	0.45	1.20	0.34	0.85	0.00	0.29	0.00	2.99	0.31	2.13	1.53	1.52	1.91	1.11	1.08	0.00	2.99	18	F	A
Hymenodictyon	60	1.80	1.13	0.00	2.10	0.39	1.30	0.90	0.80	0.68	0.51	0.25	0.58	1.48	1.99	1.25	0.61	1.27	2.28	1.09	0.89	1.07	0.00	2.28	19	F	A/a
Macaranga	48	2.70	1.36	0.78	0.00	1.18	0.00	0.45	0.40	1.02	0.00	0.99	1.16	0.00	2.99	0.63	1.52	1.53	0.76	0.54	0.45	0.92	0.00	2.99	16	F	a/A
Olea	56	0.45	1.36	0.39	0.70	0.79	1.30	0.90	0.80	0.68	1.36	0.99	1.45	1.48	0.50	0.31	1.22	1.27	0.51	1.36	0.00	0.89	0.00	1.48	19	F/Me	A/a/L
SAPOTACEAE	54	0.90	1.13	1.18	0.70	1.18	0.65	0.90	0.00	0.68	1.19	1.74	1.45	0.99	1.00	0.31	0.30	2.04	0.25	0.54	0.67	0.89	0.00	2.04	19	F	A/a/L/H
Celtis	47	0.45	1.13	0.39	0.00	0.39	0.33	0.00	0.80	1.02	0.85	0.74	0.87	0.99	1.49	0.31	0.30	0.76	0.76	2.18	0.89	0.73	0.00	2.18	18	S	a
EUPHORBIACEAE	41	0.00	1.81	0.00	0.00	0.00	0.65	0.00	0.40	1.02	0.51	0.00	0.58	1.48	1.49	1.25	1.52	0.51	0.51	0.00	1.78	0.68	0.00	1.81	13	F/S	H/A/a/L
CAESALPINIACEAE	41	0.45	0.23	1.18	0.35	1.18	1.30	0.00	0.40	1.37	1.02	0.25	0.87	0.00	1.49	0.00	0.61	0.51	0.76	0.54	0.45	0.65	0.00	1.49	17	F	A
Fagara	38	0.90	0.90	0.00	0.35	0.00	0.00	0.00	1.20	2.05	1.02	0.74	1.74	1.48	0.50	0.00	0.61	0.25	0.25	0.00	0.45	0.62	0.00	2.05	14	F/S	A
Nauclea	30	0.00	0.00	0.00	0.00	0.00	0.00	0.45	0.40	0.00	0.00	0.74	1.45	1.97	0.00	1.88	0.61	1.27	1.02	0.27	0.45	0.53	0.00	1.97	11	S/F	a
Canthium venosum type	33	0.90	0.45	0.00	0.70	0.00	0.65	0.90	0.40	0.00	1.02	0.74	1.16	0.49	0.00	0.00	0.61	0.51	0.76	0.54	0.22	0.50	0.00	1.16	15	S/F	a
Pandanus	24	0.45	0.45	0.78	0.35	1.18	0.98	0.90	0.40	0.00	0.34	0.00	0.00	0.00	1.00	0.31	0.30	0.51	0.25	0.27	0.22	0.44	0.00	1.18	16	F/S	A/a
Adenia	27	0.00	0.00	0.00	0.00	0.00	0.33	0.00	0.00	5.12	0.34	0.25	0.58	0.49	0.50	0.00	0.00	0.00	0.00	0.00	0.89	0.42	0.00	5.12	8	F	a
AMARANTHACEAE-CHENOP.	25	0.45	0.23	0.00	0.35	0.39	0.33	0.45	0.00	0.34	0.85	0.00	0.58	1.48	1.00	0.00	0.61	0.76	0.00	0.00	0.67	0.42	0.00	1.48	14	S/F	a
Maytenus	20	0.45	0.45	0.39	0.00	0.39	0.98	0.45	0.40	0.00	0.17	0.50	0.00	0.00	0.00	0.00	0.61	0.51	0.00	0.82	0.45	0.33	0.00	0.98	13	S	A
Hymenocardia	23	0.45	0.23	0.00	0.00	0.00	0.33	1.80	0.40	0.34	1.70	0.74	0.00	0.00	0.00	0.00	0.00	0.00	0.00	0.54	0.00	0.33	0.00	1.80	9	S	A/a/L
Bridelia	17	0.90	0.45	0.00	0.00	0.00	0.33	0.00	0.40	0.34	0.00	0.74	0.29	0.49	0.00	0.63	0.30	0.25	0.25	0.54	0.22	0.31	0.00	0.90	14	S	L/a
Mitragyna	16	0.90	0.45	0.00	0.35	0.39	0.00	0.45	0.00	0.34	0.17	0.00	0.58	0.99	0.00	0.00	0.61	0.25	0.00	0.27	0.22	0.30	0.00	0.99	13	S/F	A/a
Aidia micrantha	16	0.00	0.45	0.00	0.35	0.00	0.00	0.45	0.00	0.00	0.17	0.00	0.29	0.99	1.00	0.63	0.61	0.25	0.51	0.00	0.22	0.30	0.00	1.00	12	S/F	A/a
Anthocleista	18	0.90	0.00	0.00	0.35	0.00	0.00	0.00	0.00	0.00	0.34	0.25	1.45	0.00	0.50	0.00	0.30	1.02	0.51	0.00	0.22	0.29	0.00	1.45	10	F/S	A
Margaritaria	16	0.45	0.00	0.00	1.05	0.39	0.33	0.90	0.40	0.34	0.34	0.00	0.29	0.00	0.00	0.00	0.00	0.25	0.00	0.27	0.45	0.27	0.00	1.05	12	S	A/a
Mareya	16	0.00	2.71	0.00	0.00	0.00	0.00	0.00	0.80	0.00	0.00	0.00	0.00	0.00	0.00	0.31	0.30	0.25	0.76	0.00	0.22	0.27	0.00	2.71	7	S	A/a
Coelocaryon	16	0.00	0.00	0.00	0.35	0.39	0.33	0.00	0.00	0.34	0.00	0.25	0.00	0.49	0.00	0.31	0.00	0.51	0.51	0.82	0.67	0.25	0.00	0.82	11	F	A
Tetracera	15	0.00	0.23	0.00	0.00	0.39	0.00	0.45	0.00	0.00	0.17	0.00	0.00	0.99	0.50	0.00	0.00	0.00	0.25	1.36	0.45	0.24	0.00	1.36	9	S	a/L
Lannea	14	0.00	0.23	0.00	0.00	0.00	0.33	0.45	0.00	0.34	0.51	0.25	0.29	0.00	0.00	0.63	0.00	0.00	0.25	0.27	0.45	0.20	0.00	0.63	11	S	A
Entada	11	0.45	0.00	0.39	0.35	0.00	0.00	0.00	0.00	0.34	0.00	0.00	0.29	0.00	0.50	0.31	0.00	0.00	0.51	0.82	0.00	0.20	0.00	0.82	9	S	a
TOTAL		100	100	100	100	100	100	100	100	100	100	100	100	100	100	100	100	100	100	100	100	100					
Base_1 (Total pollen)		368	834	629	756	714	770	699	836	871	1798	1248	1088	815	725	667	957	783	1343	1165	1308	18374					
Base_2 (Without Rhizo and Spores)		111	295	255	286	254	307	222	251	293	587	403	345	203	201	213	328	262	394	367	449	6025					
Sum (Rhizo + Spores)		257	539	374	470	460	463	477	585	578	1211	845	743	612	524	454	629	521	949	798	859	12348					
Undetermined		3	11	11	14	14	8	8	8	13	24	15	11	12	13	10	15	12	15	13	19	249					
Damaged		2	6	2	0	2	9	4	4	3	3	7	7	1	5	6	7	5	6	3	0	81					
Dynocysts		3	1	1	0	3	0	1	1	2	3	2	0	4	3	2	1	1	1	1	3	33					
%Herbs (NAP)		24	39	55	58	51	54	44	43	34	41	42	38	32	27	34	30	31	27	27	42	39					
%Arbres and Shrub (AP)		76	61	45	42	49	46	56	57	66	59	58	62	68	73	66	70	69	73	73	58	61					

Continued

Total	100	100	100	100	100	100	100	100	100	100	100	100	100	100	100	100	100	100	100	100
%Savanna	40	51	60	63	58	61	55	54	45	52	51	49	43	41	46	39	45	43	43	50	49
%Forest	60	49	40	37	42	39	45	46	55	48	49	51	57	59	54	61	55	57	57	50	51
Total	100	100	100	100	100	100	100	100	100	100	100	100	100	100	100	100	100	100	100	100	100

4.3. Pollen Diagram (1): Bioindicator Taxa and Vegetation Phases

In this study, the Late Holocene savanna optimum is defined as the time interval during which non-arboreal pollen (NAP) values consistently exceed arboreal pollen (AP) values in the CF core, indicating a sustained dominance of open herbaceous formations over forest cover.

The first pollen diagram illustrates the temporal evolution of key bioindicator taxa, including *Rhizophora*, spores, and *Podocarpus*, together with aggregated forest and savanna groups, and arboreal (AP) versus non-arboreal pollen (NAP). Throughout the core, *Rhizophora* pollen largely dominates the assemblages, with values ranging from 41.18% to 58.40% and an average of 49.71%, approximately three times higher than spore percentages (Figure 5).

Although *Rhizophora* and spore curves show partially contrasting trends, spores remain consistently subordinate. *Podocarpus* pollen occurs in very low proportions (<1%) and does not provide robust quantitative information. In contrast, combined forest-savanna and AP/NAP curves reveal three distinct Late Holocene vegetation phases, defined by intersections of the respective curves (Figure 5).

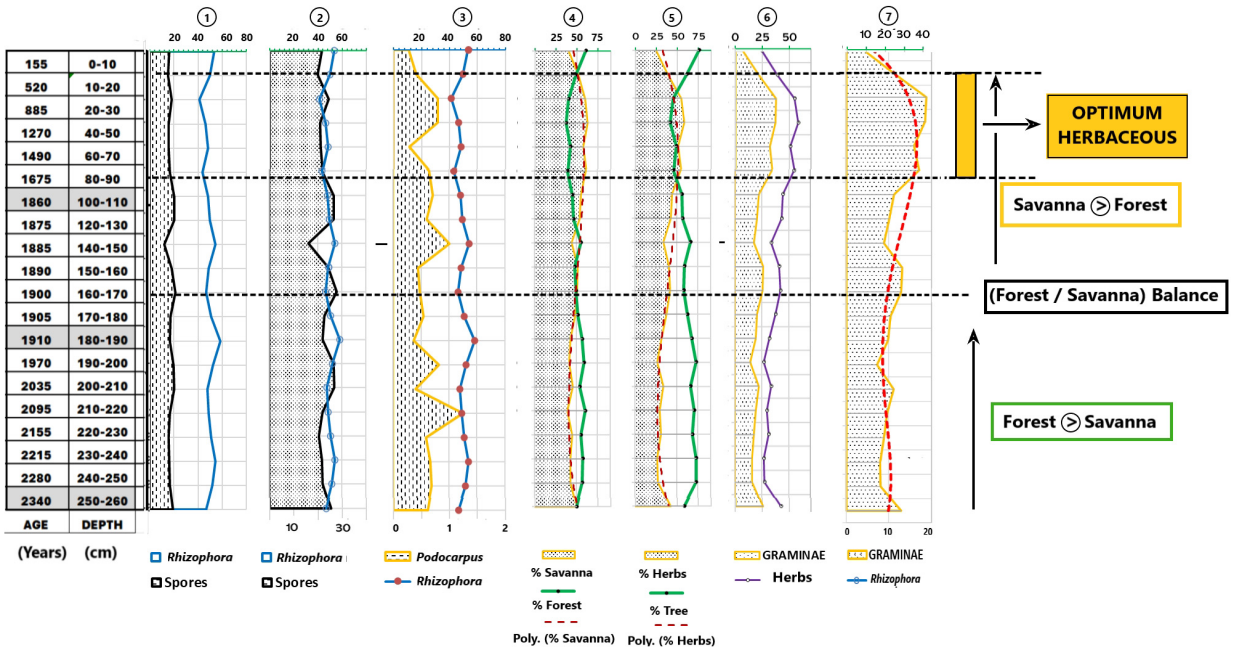

Figure 5. Diagram (1) vegetation types and ecological bioindicators.

Phase 1, recorded in the lower section of the core (260 cm - 160 cm; ~2,340 - 1,900 cal yr BP), is characterized by the dominance of arboreal pollen and forest taxa.

Phase 2, extending from ~160 to 20 cm and lasting until about 885 cal yr BP, shows a marked expansion of savanna and herbaceous taxa. The uppermost metre of the core corresponds to a pronounced herbaceous savanna optimum, with AP/NAP ratios strongly favoring non-arboreal pollen. Phase 3 reflects a gradual recovery of arboreal taxa and forest formations during the most recent centuries (Figure 5).

The overall trend indicates a progressive increase in herbaceous taxa upward through the sequence. A strong correlation between grass (Poaceae) and savanna curves supports the use of Poaceae as a reference proxy for tracking savanna dynamics and for comparison with other ecosystem-specific taxa (Figure 5).

4.4. Pollen Diagram (2): Major Ecosystem Taxa

The second pollen diagram focuses on major taxa representative of key ecosystems, using Poaceae as the primary paleoenvironmental and climatic indicator (Figure 6). Savanna-related taxa such as Cyperaceae and *Commelina*, forest taxa including Caesalpiniaceae, Sapotaceae, and *Pycnanthus*, pioneer and ubiquitous taxa (*Alchornea*, *Uapaca*, *Elaeis*), as well as taxa indicative of specific environments (*Rhizophora* for mangroves and *Podocarpus* for montane vegetation), are displayed (Figure 6).

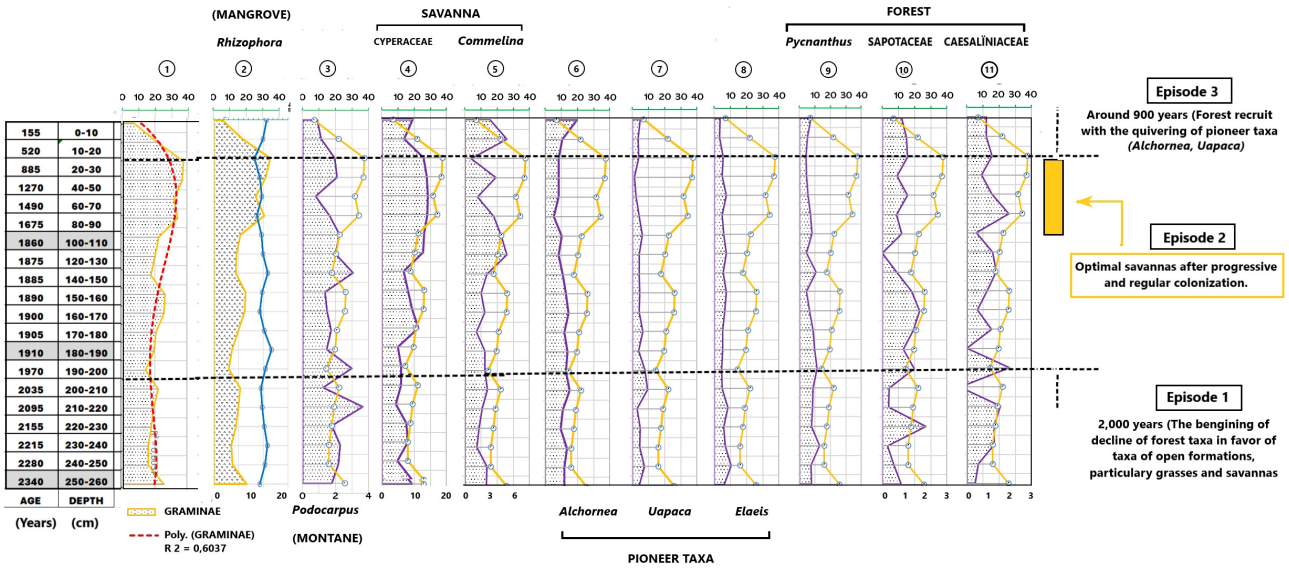

Figure 6. Diagram (2) composite pollen diagram of the main taxa.

The Poaceae curve shows three distinct phases: an initial interval with relatively stable values around 7% between ~2,340 and 2,000 cal yr BP; a phase of gradual increase culminating in a maximum of approximately 15% corresponding to the Late Holocene savanna optimum; and a subsequent decline to values near 2% after ~900 cal yr BP (Figure 6). Cyperaceae and *Commelina* display trends similar to those of Poaceae, with pronounced peaks in the upper part of the core (Figure 6).

Pioneer taxa (*Alchornea*, *Uapaca*, *Elaeis*) are consistently present throughout the sequence, with increased abundances toward the top of the core as Poaceae

values decrease (Figure 6). Forest taxa (*Pycnanthus*, Sapotaceae, Caesalpiniaceae) generally remain below 3% and show declining trends during the savanna expansion phase. *Pycnanthus* exhibits a clear inverse relationship with Poaceae, while *Podocarpus* remains rare and sporadic (Figure 6). An inverse relationship is also observed between Poaceae and *Rhizophora*, reflecting opposing dynamics between savanna expansion and mangrove development (Figure 6).

4.5. Correspondence Factor Analysis

Correspondence factor analysis (CFA), based on active variables including the main pollen taxa and ecological groups representative of forest (e.g., Caesalpiniaceae, Sapotaceae, *Pycnanthus*), savanna (Poaceae, Cyperaceae), pioneer (*Alchornea*, *Uapaca*, *Elaeis*), mangrove (*Rhizophora*), and Afro-montane (*Podocarpus*) vegetation, identifies three main groups of samples (Figure 7). Axis 1 reflects a linear and progressive shift from the lower to the upper sections of the core, consistent with variations observed in forest-savanna and AP/NAP ratios (Figure 7). The first group comprises samples from the basal part of the core (180 cm - 250 cm), characterized by high proportions of forest taxa and minimal savanna representation (Figure 7).

The second group occupies an intermediate position and includes samples with comparable proportions of forest and savanna taxa. The third group corresponds to upper-core samples (20 cm - 90 cm), dominated by savanna and herbaceous taxa (Figure 7). This multivariate structure confirms the gradual Late Holocene transition from forest-dominated to savanna-dominated landscapes and the subsequent partial forest recovery (Figure 7).

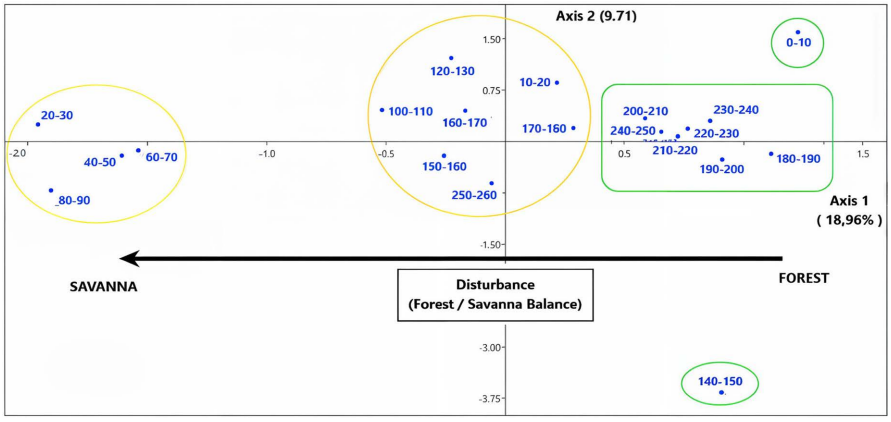

Figure 7. Correspondence factor analysis: gradual reduction of the forest to savannah.

5. Discussion

5.1. Taxonomic Diversity and Pollen Signal Representativeness

The pollen assemblages of core CF display a high taxonomic diversity, reflecting both the variety of plant formations present in the drainage basins and the efficiency of pollen transport from continent to shelf. The dominance of *Rhizophora*,

followed by spores, Poaceae, Cyperaceae, *Alchornea*, *Elaeis*, *Drypetes*, *Uapaca*, and *Podocarpus* (**Table 1**), closely matches the spectra observed in recent surface sediments collected near the CF site (Bengo et al., 2025a). This similarity highlights the strong influence of fluvial inputs—primarily from the Sanaga River—and tidal dynamics within the Bays of Douala and Rio del Rey on the pollen signal.

The upper part of the CF core, therefore, records a pollen rain representative of the modern vegetation mosaic at the scale of the Sanaga watershed, which crosses most of Cameroon's major ecological zones, from humid evergreen forests in the south to savannas in the central and northern regions (Bengo et al., 2020). Comparable relationships between riverine pollen transport and watershed-scale vegetation have been documented elsewhere in the Gulf of Guinea (Fredoux & Maley, 1996). Consequently, variations observed along the CF sequence are interpreted as reflecting genuine changes in vegetation physiognomy and environmental conditions, driven by shifts in key climatic parameters such as temperature, precipitation, potential evapotranspiration, and moisture balance.

5.2. Paleoecological Bioindicators and Climatic Significance

Marine palynological records spanning long time intervals commonly exhibit high and variable proportions of spores, *Rhizophora*, *Podocarpus*, and Poaceae, making these taxa robust indicators of environmental change. However, the CF core documents only the last ~2,500 years of the Late Holocene and corresponds to a restricted segment of the broader palynological phases identified in the offshore C61 core. Within this temporal window, the CF record indicates relative stability, albeit with fluctuations, in the proportions of major bioindicators such as *Rhizophora*, spores, and *Podocarpus* (**Figure 5**).

High percentages of *Rhizophora* pollen are characteristic of Late Holocene marine records throughout the Gulf of Guinea, including sequences from Gabon (GIK16867; Dupont et al., 1998), Congo (GeoB1008; Jahns, 1996; Bengo & Maley, 1991), and Angola (GeoB1016; Shi & Dupont, 1997). Such values reflect both the extensive development of mangrove ecosystems along tropical coasts and the strong dispersal capacity of *Rhizophora* pollen in marine environments. Occasional occurrences of *Rhizophora* in lagoonal and even continental sediments have also been reported, particularly in the Niger Delta region, due to alluvial transport (Sowunmi, 1987; Malounguila et al., 2017).

In contrast, spores show a relative decrease of about one-third through the CF sequence, while *Rhizophora* values increase by a factor of three. Despite some opposing short-term variations, spores remain consistently less abundant than *Rhizophora*, suggesting that coastal environments remained relatively stable during the Late Holocene. A marked decline in Afro-montane taxa, especially *Podocarpus*, is also evident, with values decreasing from nearly 11% to less than 1% (Bengo, 1996; Reynaud-Farrera et al., 1996). This pattern mirrors observations from numerous continental lake records across Cameroon and Central Africa.

The disappearance or strong reduction of *Podocarpus* is a recurrent feature of

Late Holocene pollen records. At Lake Ossa, *Podocarpus* was still present around 2,730 cal yr BP but vanished by ~950 cal yr BP (Reynaud-Farrera et al., 1996). Similar declines are documented at Lake Barombi-Mbo between ~4,000 and 2,000 cal yr BP (Brenac, 1988; Maley & Brenac, 1998), at Lake Bambili, where *Podocarpus* dropped from ~30% to less than 2% after ~2,000 cal yr BP (Assi-Kaudjhis et al., 2008; Assi-Kaudjhis et al., 2010; Assi-Kaudjhis, 2012), and at Lake Njupi, where it disappeared around 2,300 cal yr BP (Zogning et al., 1997). Comparable trends are observed at Lake Mbalang (Vincens et al., 2010), Lake Mboandong (Richards, 2021), and sites on the Bateke Plateau (Elenga & Vincens, 1990).

Podocarpus is typically associated with cool and humid montane environments, generally above 1,000 m elevation, where frequent fog and cloud cover provide occult precipitation—conditions characteristic of so-called "cloud forests" (Kerfoot, 1968). Its widespread decline during the Late Holocene, therefore, suggests a regional shift toward warmer and/or drier conditions at mid and low altitudes. Conversely, such conditions would have favored the expansion of mangrove ecosystems, as *Rhizophora* requires mean temperatures above ~22˚C (Din, 1991). The CF marine record thus supports the hypothesis that the end of the Middle Holocene was marked by cooling episodes sufficient to allow the downslope expansion of montane taxa, followed by Late Holocene warming that restricted these taxa to higher elevations.

5.3. Late Holocene Forest-Savanna Dynamics

Analysis of grouped forest versus savanna taxa and arboreal (AP) versus non-arboreal pollen (NAP) curves (**Figure 5**) reveals three main phases of vegetation change during the Late Holocene. The first phase, from the base of the core (~2,340 cal yr BP) to ~1,900 cal yr BP, is characterized by a dominance of forest taxa and arboreal pollen. The first intersection of forest and savanna curves marks a transition toward more open landscapes. A second intersection, occurring around ~520 years before present, defines the onset of a third phase characterized by renewed forest development.

Data from the offshore C61 core indicate that forest degradation may have begun earlier, around ~3,200 cal yr BP, with gradual replacement of forest species by pioneer taxa and increasing savanna elements (Bengo, 1996; Bengo et al., 2025b). Periods when forest and savanna proportions are similar likely correspond to wooded or shrub savannas, whereas intervals dominated by herbaceous pollen reflect grassy savannas. Between ~1,675 and 885 cal yr BP, NAP values exceed AP values, defining a pronounced Late Holocene "savanna optimum," during which grasslands expanded at the expense of forest cover.

The polynomial trend of Poaceae (**Figure 6**) also distinguishes three stages: an initial phase of relative equilibrium until ~2,000 cal yr BP, a prolonged phase of increase culminating in a plateau between ~1,675 and 885 cal yr BP, and a final phase marked by grass decline and partial forest recovery toward the present. These trends confirm the usefulness of Poaceae as a proxy for tracking savanna

dynamics in marine records.

5.4. Regional Perspective on Savanna Dynamics in Central and Equatorial Africa

Comparison of the CF pollen record with continental sequences across Central and Equatorial Africa reveals coherent regional patterns of savanna expansion and contraction during the Late Holocene. In Equatorial Africa, Lake Sélé records two major grass peaks around ~3,300 and ~850 cal yr BP, with increased values near ~2,000 cal yr BP (Salzmann & Hoelzmann, 2005). In Congo, sites such as Bilanko, Sinnda, and Kitina document late and often abrupt grass expansions after ~2,500 cal yr BP (Elenga & Vincens, 1990; Vincens et al., 1994; Elenga et al., 1996).

In Gabon, grass pollen remains consistently present at Lake Kamalaté and Lake Maridor, indicating relatively stable conditions favorable to herbaceous formations, whereas Lake Nguène shows a marked resurgence of grasses after ~2,000 cal yr BP (Ngomanda et al., 2005; Giresse et al., 2009; Giresse et al., 2020). In Cameroon, lacustrine records from Mbalang, Tizong, Barombi-Mbo, Njupi, Bambili, and Ossa all document significant grass expansions between ~2,500 and 1,000 cal yr BP, broadly synchronous with the savanna optimum identified in the CF core.

The similarity between the CF marine record and lacustrine sequences from low-altitude (Ossa) and high-altitude (Bambili) sites suggests a regional-scale driver affecting vegetation dynamics. The continuous grass expansion from ~2,000 cal yr BP to a maximum between ~1,600 and 900 cal yr BP likely reflects the combined effects of hydroclimatic variability, cooling-warming oscillations, and shoreline and hydrological changes that altered ecosystem resilience across Central Africa.

5.5. Forest Dynamics, Pioneer Taxa, and Human Influence

The increase in *Elaeis guineensis* pollen values during the Late Holocene has traditionally been interpreted as an indirect indicator of early human activities in Central Africa. Numerous studies have linked the expansion of *Elaeis* to forest opening by agro-pastoral societies, particularly in the context of Bantu migrations, during which oil palm populations may have been favored through land clearing, fire use, and selective protection or management (De Maret et al., 1987; Maley et al., 2018). Within this framework, *Elaeis* is commonly regarded as a robust palynological marker of Holocene anthropogenic disturbance.

However, the signal recorded in the CF core calls for a more nuanced interpretation. Although *Elaeis* is consistently present throughout the sequence and increases in parallel with phases of landscape opening and the development of pioneer taxa, its marked decline in the most recent levels contrasts with the expectation of a continuous or intensified expansion under increasing human pressure. Similar trends have been reported from several continental records in the region (e.g., Ossa, Mboandong, Kitina), suggesting that the relationship between human activities and *Elaeis* dynamics is neither linear nor uniform through time.

This recent decline may reflect qualitative changes in land-use practices, dis-

tinct from earlier Holocene disturbances. Potential modern drivers include: i) agricultural policies and practices promoting cash crops or food crops that compete with naturally regenerating oil palm, ii) land-use intensification (mechanized agriculture, shortening of fallow periods, urban expansion) leading to reduced opportunities for *Elaeis* recruitment, and iii) increased and sometimes selective exploitation of oil palms, potentially resulting in local depletion of natural stands.

Consequently, while the earlier expansion of *Elaeis* appears compatible with diffuse anthropogenic disturbances integrated within natural successional processes, its recent decline suggests a stronger and more structurally transformative human pressure, possibly exceeding ecosystem resilience thresholds. In this sense, the *Elaeis* signal in the CF record emerges as a sensitive indicator of the transition from extensive, low-intensity human-environment interactions to more intensive and potentially degrading modern land-use systems.

6. Conclusion

The CF marine core, collected at 38 m water depth off the Bay of Douala, provides a continuous and well-constrained record of environmental change over the last ~2,500 years of the Late Holocene on the Cameroonian continental shelf. Palynological analysis documents a high diversity with 228 taxa belonging to 90 plant families, and assemblages dominated by *Rhizophora* pollen, followed by spores, Poaceae, *Alchornea*, Cyperaceae, and *Elaeis*.

The CF record identifies three major vegetation phases: 1) an initial forest-dominated phase from ~2,340 to ~1,900 cal yr BP; 2) a marked expansion of open herbaceous formations culminating in a Late Holocene savanna optimum between ~1,600 and 900 cal yr BP; and 3) a phase of partial forest recovery after ~885 cal yr BP, driven mainly by pioneer taxa. Correspondence factor analysis confirms a progressive shift from lower to upper core samples consistent with forest-savanna and AP/NAP variations.

Beyond its paleoenvironmental significance, the CF record provides a quantitative basis for anticipating future ecosystem trajectories under ongoing climate change: the well-dated shifts in the forest-savanna boundary constrain the pace, direction and potential thresholds of vegetation change, offering empirical benchmarks to calibrate and validate dynamic vegetation and Earth system models and to improve projections of forest-savanna resilience and possible biome reorganization under future climate scenarios.

Conflicts of Interest

The authors declare no conflicts of interest regarding the publication of this paper.

References

Aloisi, J. C., Benkhelil, J., Giresse, P., & Ngueutchoua, G. (1995). Étude sismique haute résolution du précontinent sud-camerounais: Analyses faciologique et structurale. *Comptes Rendus de l'Académie des Sciences, Série IIa, 321,* 145-152.

Assi-Kaudjhis, C. (2012). *Dynamique des écosystèmes et biodiversité des montagnes du*

Cameroun au cours des derniers 20 000 ans: Analyse palynologique d'une série sédimentaire du Lac Bambili. Thesis, Université de Liège and Université de Versailles Saint-Quentin-en-Yvelines.

Assi-Kaudjhis, C., Lézine, A.-M., & Roche, E. (2008) Dynamique de la végétation d'altitude en Afrique centrale atlantique depuis 17 000 ans BP: Analyses préliminaires de la carotte de Bambili (Nord-Ouest du Cameroun). *Geo-Eco-Trop, 32,* 131-143.

Assi-Kaudjhis, C., Zéli Digbehi, B., Roche, E., & Lézine, A.-M. (2010) Synthèse sur l'évolution des paléoenvironnements de l'Afrique occidentale atlantique depuis la fin de la dernière période glaciaire: Influences climatiques et anthropiques. *Geo-Eco-Trop, 34,* 1-28.

Bengo, M. D. (1996). *La sédimentation pollinique dans le Sud-Cameroun et sur la plateforme marine à l'époque actuelle et au Quaternaire récent: Études des paléoenvironnements*. Master's Thesis, Université Montpellier 2.

Bengo, M. D., & Maley, J. (1991). Analyses des flux polliniques sur la marge sud du Golfe de Guinée depuis 135000 ans. *Comptes Rendus de l'Académie des Sciences de Paris, Série II, 313,* 843-849.

Bengo, M. D., Elenga, H., Maley, J., & Giresse, P. (2020). Evidence of Pollen Transport by the Sanaga River on the Cameroon Shelf. *Comptes Rendus. Géoscience, 352,* 59-72. https://doi.org/10.5802/crgeos.1

Bengo, M. D., Gomat, H., Giresse, P., Maley, J., & Nganga, D. M. (2025a). Implications of Marine Hydrodynamism in the Dispersal and Modern Distribution of Pollen on the Cameroonian Continental Shelf. *Open Journal of Geology, 15,* 716-734. https://doi.org/10.4236/ojg.2025.1510035

Bengo, M. D., Gomat, H., Ifo, S. A., Maley, J., & Giresse, P. (2025b). Late Quaternary Paleoenvironmental Dynamics on the Cameroonian Continental Shelf (Gulf of Guinea): Palynological and Sedimentary Insights. *Journal of Geoscience and Environment Protection, 13,* 92-115. https://doi.org/10.4236/gep.2025.1312006

Bonnefille, R., & Riollet, G. (1980). *Pollens des savanes d'Afrique orientale* (pp. 113-130). CNRS.

Bourles, B., Molinari, R. L., Johns, E., Wilson, W. D., & Leaman, K. D. (1999). Upper Layer Currents in the Western Tropical North Atlantic (1989-1991). *Journal of Geophysical Research: Oceans, 104,* 1361-1375. https://doi.org/10.1029/1998jc900025

Boyé, M., Baltzer, F., Caratini, C., Hampartzoumian, A., Olivry, J. C., Plaziat, J. C., & Villiers, J. F. (1975) Mangrove of the Wouri Estuary, Cameroon. In G. E. Walsh, S. C. Snedaker, & H. J. Teas (Eds.), *Proceedings of the International Symposium on Biology and Management of Mangroves* (Vol. 2, pp. 431-454). Institute of Food and Agricultural Sciences, University of Florida.

Braga, E. S., Andrié, C., Bourlès, B., Vangriesheim, A., Baurand, F., & Chuchla, R. (2004). Congo River Signature and Deep Circulation in the Eastern Guinea Basin. *Deep Sea Research Part I: Oceanographic Research Papers, 51,* 1057-1073. https://doi.org/10.1016/j.dsr.2004.03.005

Bremond, L., Favier, C., Ficetola, G. F., Tossou, M. G., Akouégninou, A., Gielly, L. et al. (2017). Five Thousand Years of Tropical Lake Sediment DNA Records from Benin. *Quaternary Science Reviews, 170,* 203-211. https://doi.org/10.1016/j.quascirev.2017.06.025

Brenac, P. (1988). Évolution de la végétation et du climat de l'Ouest-Cameroun entre 25 000 et 11 000 ans BP. *Travaux de la Section Scientifique et Technique de l'Institut Français de Pondichéry, 25,* 91-103.

Brncic, T. M., Willis, K. J., Harris, D. J., Telfer, M. W., & Bailey, R. M. (2009). Fire and Climate Change Impacts on Lowland Forest Composition in Northern Congo during the

Last 2580 Years from Palaeoecological Analyses of a Seasonally Flooded Swamp. *The Holocene, 19,* 79-89. https://doi.org/10.1177/0959683608098954

De Maret, P., Clist, B., & Van Neer, W. (1987). Résultats des premières fouilles dans les abris sous roche de Shum Laka et d'Abeke au Nord-Ouest du Cameroun. *L'Anthropologie, 91,* 559-584.

Din, D. (1991). *Contribution à l'étude botanique et écologique des mangroves de l'estuaire du Cameroun*. Thesis, University of Yaoundé.

Dupont, L. M., & Weinelt, M. (1996). Vegetation History of the Savanna Corridor between the Guinean and the Congolian Rain Forest during the Last 150,000 Years. *Vegetation History and Archaeobotany, 5,* 273-292. https://doi.org/10.1007/bf00195296

Dupont, L. M., Marret, F., & Winn, K. (1998). Land-Sea Correlation by Means of Terrestrial and Marine Palynomorphs from the Equatorial East Atlantic: Phasing of SE Trade Winds and the Oceanic Productivity. *Palaeogeography, Palaeoclimatology, Palaeoecology, 142,* 51-84. https://doi.org/10.1016/s0031-0182(97)00146-6

Elenga, H., & Vincens, A. (1990). Paléoenvironnements quaternaires récents des plateaux Bateke (Congo): Étude palynologique des dépôts de la dépression du bois de Bilanko. In R. Lanfranchi, & D. Schwartz (Eds.), *Paysages quaternaires de l'Afrique centrale atlantique* (pp. 271-282). ORSTOM.

Elenga, H., Schwartz, D., Vincens, A., Bertaux, J., De Namur, C., Martin, L., Wirrmann, D., & Servant, M. (1996). Diagramme pollinique holocène du lac Kitina (Congo): Mise en évidence de changements paléobotaniques et paléoclimatiques dans le massif forestier du Mayombe. *Comptes Rendus de l'Académie des Sciences de Paris, 323,* 403-410.

Faegri, K., & Iversen, J. (1992). *Textbook of Pollen Analysis* (4th ed.). Blackwell Scientific Publications.

Fredoux, A. (1994). Paléoenvironnements enregistres dans une carotte marine du golfe de Guinée depuis 225 000 ans: Analyse pollinique. In R. Maire, S. Pomel, & J. N. Salomon (Eds.), *Enregistreurs et indicateurs de l'évolution de l'environnement en zone tropicale* (pp. 85-102). Presses Universitaires de Bordeaux. https://doi.org/10.4000/books.pub.9929

Fredoux, A., & Maley, J. (1996) Le contenu pollinique de l'atmosphère dans les forêts sud-camerounaises près de Yaoundé. In *Dynamique à long terme des écosystèmes forestiers intertropicaux* (p. 63). ORSTOM.

Giresse, P., Aloisi, J., Kuete, M., Monteillet, J., & Ngueutchoua, G. (1995). Quaternary Sedimentary Deposits on the Cameroon Shelf: Characterization of Facies and Late Quaternary Shorelines. *Quaternary International, 29,* 75-87. https://doi.org/10.1016/1040-6182(95)00009-8

Giresse, P., Maley, J., & Chepstow-Lusty, A. (2020). Understanding the 2500 Yr BP Rainforest Crisis in West and Central Africa in the Framework of the Late Holocene: Pluridisciplinary Analysis and Multi-Archive Reconstruction. *Global and Planetary Change, 192,* Article ID: 103257. https://doi.org/10.1016/j.gloplacha.2020.103257

Giresse, P., Maley, J., & Kossoni, A. (2005). Sedimentary Environmental Changes and Millennial Climatic Variability in a Tropical Shallow Lake (Lake Ossa, Cameroon) during the Holocene. *Palaeogeography, Palaeoclimatology, Palaeoecology, 218,* 257-285. https://doi.org/10.1016/j.palaeo.2004.12.018

Giresse, P., Mvoubou, M., Maley, J., & Ngomanda, A. (2009). Late-Holocene Equatorial Environments Inferred from Deposition Processes, Carbon Isotopes of Organic Matter, and Pollen in Three Shallow Lakes of Gabon, West-Central Africa. *Journal of Paleolimnology, 41,* 369-392. https://doi.org/10.1007/s10933-008-9231-5

Intergovernmental Panel on Climate Change (IPCC) (2021). *Climate Change 2021—The*

Physical Science Basis: Contribution of Working Group I to the Sixth Assessment Report of the Intergovernmental Panel on Climate Change. Cambridge University Press.

Jahns, S. (1996). Vegetation History and Climate Changes in West Equatorial Africa during the Late Pleistocene and Holocene, Based on a Marine Pollen Diagram from the Congo Fan. *Vegetation History and Archaeobotany, 5,* 207-213. https://doi.org/10.1007/bf00217498

Jahns, S., Hüls, M., & Sarnthein, M. (1998). Vegetation and Climate History of West Equatorial Africa Based on a Marine Pollen Record off Liberia (Site GIK 16776) Covering the Last 400,000 Years. *Review of Palaeobotany and Palynology, 102,* 277-288. https://doi.org/10.1016/s0034-6667(98)80010-9

Julier, A. C. M., Jardine, P. E., Adu-Bredu, S., Coe, A. L., Duah-Gyamfi, A., Fraser, W. T. et al. (2018). The Modern Pollen-Vegetation Relationships of a Tropical Forest-Savannah Mosaic Landscape, Ghana, West Africa. *Palynology, 42,* 324-338. https://doi.org/10.1080/01916122.2017.1356392

Kerfoot, O. (1968). Mist Precipitation on Vegetation. *Oxford Forestry Abstracts, 29,* 8-20.

Kiahtipes, C., & Schefuß, E. (2018). *Congo Basin Peatlands as Baseline Records for Past Hydrology and Climate*. AGU Chapman Conference (Poster W68). https://doi.org/10.1002/essoar.10500726.1

Kolodziejczyk, N. (2008). *Analyse de la circulation de subsurface et de sa variabilité dans le Golfe de Guinée*. Ph.D. Thesis, Université de Bretagne Occidentale. https://theses.fr/2008BRES2020

Lebamba, J., Vincens, A., & Maley, J. (2012). Pollen, Vegetation Change and Climate at Lake Barombi Mbo (Cameroon) during the Last Ca. 33 000 Cal yr BP: A Numerical Approach. *Climate of the Past, 8,* 59-78. https://doi.org/10.5194/cp-8-59-2012

Leroux, M. (1983). *Le climat de l'Afrique tropicale* (Vols. 1-2). Champion.

Letouzey, R. (1968). *Étude phytogéographique du Cameroun*. Lechevalier.

Lézine, A.-M., & Cazet, J. (2005). High-Resolution Pollen Record from Core KW31, Gulf of Guinea, Documents the History of the Lowland Forests of West Equatorial Africa since 40,000 yr Ago. *Quaternary Research, 64,* 432-443. https://doi.org/10.1016/j.yqres.2005.08.007

Lézine, A.-M., & Vergnaud-Grazzini, C. (1993). Evidence of Forest Extension in West Africa since 22,000 BP: A Pollen Record from the Eastern Tropical Atlantic. *Quaternary Science Reviews, 12,* 203-210. https://doi.org/10.1016/0277-3791(93)90054-p

Mahé, G., & Olivry, J.-C. (1991) Changements climatiques et variations des écoulements en Afrique occidentale et centrale, du mensuel à l'interannuel. In *Hydrology for the Water Management of Large River Basins (Proceedings of the Vienna Symposium, August 1991)* (pp. 163-171). IAHS Publication.

Maley, J. (1970). Contributions a l'etude du Bassin tchadien Atlas de pollens du Tchad. *Bulletin du Jardin Botanique National de Belgique, 40,* 29-48. https://doi.org/10.2307/3667543

Maley, J. (1991). The African Rain Forest Vegetation and Palaeoenvironments during Late Quaternary. *Climatic Change, 19,* 79-98. https://doi.org/10.1007/bf00142216

Maley, J., & Brenac, P. (1998). Vegetation Dynamics, Palaeoenvironments and Climatic Changes in the Forests of Western Cameroon during the Last 28,000 Years B.P. *Review of Palaeobotany and Palynology, 99,* 157-187. https://doi.org/10.1016/s0034-6667(97)00047-x

Maley, J., & Willis, K.J. (2010). *Did a Savanna Corridor Open up across the Central African Forests 2500 Years Ago*? CoForChange Letter, 2.

Maley, J., Doumenge, C., Giresse, P., Mahé, G., Philippon, N., Hubau, W. et al. (2018). Late Holocene Forest Contraction and Fragmentation in Central Africa. *Quaternary Research, 89,* 43-59. https://doi.org/10.1017/qua.2017.97

Malhi, Y., Gardner, T. A., Goldsmith, G. R., Silman, M. R., & Zelazowski, P. (2014). Tropical Forests in the Anthropocene. *Annual Review of Environment and Resources, 39,* 125-159. https://doi.org/10.1146/annurev-environ-030713-155141

Malounguila-Nganga, D., Giresse, P., Boussafir, M., & Miyouna, T. (2017). Late Holocene Swampy Forest of Loango Bay (Congo). Sedimentary Environments and Organic Matter Deposition. *Journal of African Earth Sciences, 134,* 419-434. https://doi.org/10.1016/j.jafrearsci.2017.05.022

Marret, F., Kim, S., & Scourse, J. (2013). A 30,000 yr Record of Land-Ocean Interaction in the Eastern Gulf of Guinea. *Quaternary Research, 80,* 1-8. https://doi.org/10.1016/j.yqres.2013.04.003

Martin, D. (1966). *Études pédologiques dans le Centre Cameroun (Nanga-Eboko à Bertoua).* Mémoire ORSTOM, No. 19, ORSTOM.

Moyersons, I. (1996). Evolution of the Shum Laka Rock Shelter (Western Cameroon) since Late Stone Age Times. In *Aspects of African Archaeology. Papers from the 10th Congress of the Pan-African Association for Prehistory and Related Studies* (pp. 245-255). University of Zimbabwe Publications.

Ngomanda, A., Chepstow-Lusty, A., Makaya, M., Favier, C., Schevin, P., Maley, J. et al. (2009a). Western Equatorial African Forest-Savanna Mosaics: A Legacy of Late Holocene Climatic Change? *Climate of the Past, 5,* 647-659. https://doi.org/10.5194/cp-5-647-2009

Ngomanda, A., Chepstow-Lusty, A., Makaya, M., Schevin, P., Maley, J., Fontugne, M. et al. (2005). Vegetation Changes during the Past 1300 Years in Western Equatorial Africa: A High Resolution Pollen Record from Lake Kamalee, Lope Reserve, Central Gabon. *The Holocene, 15,* 1021-1031. https://doi.org/10.1191/0959683605hl875ra

Ngomanda, A., Neumann, K., Schweizer, A., & Maley, J. (2009b). Seasonality Change and the Third Millennium BP Rainforest Crisis in Southern Cameroon (Central Africa). *Quaternary Research, 71,* 307-318. https://doi.org/10.1016/j.yqres.2008.12.002

Nguetsop, V. F., Servant-Vildary, S., Servant, M., & Roux, M. (2010). Long and Short-Time Scale Climatic Variability in the Last 5500 Years in Africa According to Modern and Fossil Diatoms from Lake Ossa (Western Cameroon). *Global and Planetary Change, 72,* 356-367. https://doi.org/10.1016/j.gloplacha.2010.01.011

Ngueutchoua, G. (1996). *Étude des faciès et environnements sédimentaires du Quaternaire supérieur du plateau continental camerounais*. Master's Thesis, Université de Perpignan Via Domitia.

Ngueutchoua, G., & Giresse, P. (2010). Sand Bodies and Incised Valleys within the Late Quaternary Sanaganyong Delta Complex on the Middle Continental Shelf of Cameroon. *Marine and Petroleum Geology, 27,* 2173-2188. https://doi.org/10.1016/j.marpetgeo.2010.06.011

Piton, B. (1987). Les anomalies océanographiques et climatiques de 1983 et 1984 dans le Golfe de Guinée. *Veille Climatique Satellitaire, 16,* 18-31.

Reynaud-Farrera, I., Maley, J., & Wirrmann, D. (1996). Végétation et climat dans les forêts du Sud-Ouest camerounais depuis 4770 ans BP: Analyse pollinique des sédiments du lac Ossa. *Comptes Rendus de l'Académie des Sciences de Paris, Série IIa, 322,* 749-755.

Richards, K. (2021). A Holocene Pollen Record from Mboandong, a Crater Lake in Lowland Cameroon. In *Quaternary Vegetation Dynamics—The African Pollen Database* (pp. 207-224). CRC Press. https://doi.org/10.1201/9781003162766-13

Riding, J. B. (2021). A Guide to Preparation Protocols in Palynology. *Palynology, 45,* 1-110. https://doi.org/10.1080/01916122.2021.1878305

Salard-Cheboldaeff, M. (1980). Cameroonian Palynology. I. Pollen from Mangroves and Coastal Shrub Thickets. In *Comptes Rendus du 105e Congrès National des Sociétés Savantes* (Vol. 1, pp. 233-247). Bibliothèque nationale de France.

Salard-Cheboldaeff, M. (1981). Cameroonian Palynology. II. Pollen Grains from Low-Altitude Coastal Forest. In *Comptes Rendus du 106e Congrès National des Sociétés Savantes* (Vol. 1, pp. 125-136). Bibliothèque nationale de France.

Salard-Cheboldaeff, M. (1982). Cameroonian Palynology. Pollen Grains from the Dense Humid Forest of Low and Medium Altitudes. In *Comptes Rendus du 107e Congrès National des Sociétés Savantes* (Vol. 1, pp. 127-141). Bibliothèque nationale de France.

Salard-Cheboldaeff, M. (1983). Cameroonian Palynology. Pollen Grains from the Dense Humid Forest of Medium Altitude. In *Comptes Rendus du 108e Congrès National des Sociétés Savantes* (Vol. 2, pp. 117-129). Bibliothèque nationale de France.

Salzmann, U., & Hoelzmann, P. (2005). The Dahomey Gap: An Abrupt Climatically Induced Rain Forest Fragmentation in West Africa during the Late Holocene. *The Holocene, 15,* 190-199. https://doi.org/10.1191/0959683605hl799rp

Salzmann, U., Hoelzmann, P., & Morczinek, I. (2002). Late Quaternary Climate and Vegetation of the Sudanian Zone of Northeast Nigeria. *Quaternary Research, 58,* 73-83. https://doi.org/10.1006/qres.2002.2356

Segalen, P. (1967). Les sols et la géomorphologie du Cameroun. *Cahiers ORSTOM, Série Pédologie, 5,* 137-188.

Shi, N., & Dupont, L. M. (1997). Vegetation and Climatic History of Southwest Africa: A Marine Palynological Record of the Last 300,000 Years. *Vegetation History and Archaeobotany, 6,* 117-131. https://doi.org/10.1007/bf01261959

Sowunmi, M. A. (1987). Palynological Studies in the Niger Delta. In E. J. Alagoa, F. N. Anozie, & N. Nzewunwa (Eds.), *The Early History of the Niger Delta* (pp. 29-64). University of Port Harcourt.

Suchel, J.-B. (1988). *Les climats du Cameroun*. Master's Thesis, Université de Saint-Étienne.

Vincens, A., Buchet, G., & Servant, M. (2010). Vegetation Response to the "African Humid Period" Termination in Central Cameroon (7˚N)—New Pollen Insight from Lake Mbalang. *Climate of the Past, 6,* 281-294. https://doi.org/10.5194/cp-6-281-2010

Vincens, A., Buchet, G., Elenga, H., Fournier, M., Martin, L., Namur, C., Schwartz, D., Servant, M., & Wirrmann, D. (1994) Changement majeur de la végétation du lac Sinnda (Vallée du Niari, sud-Congo) consécutif à l'assèchement climatique holocène su-périeur: Apport de la palynologie. *Comptes Rendus de l'Académie des Sciences de Paris, 318,* 1521-1526.

Zogning, A., Giresse, P., Maley, J., & Gadel, F. (1997). The Late Holocene Palaeoenvironment in the Lake Njupi Area, West Cameroon: Implications Regarding the History of Lake Nyos. *Journal of African Earth Sciences, 24,* 285-300. https://doi.org/10.1016/s0899-5362(97)00044-4